1-1-2018

Allicin- inspired pyridyl disulfides as antimicrobial agents for multidrug-resistant Staphylococcus aureus

Jordan G. Sheppard
Marshall University

Jeremy P. McAleer
Marshall University

Pushkar Saralkar
West Virginia University

Werner J. Geldenhuys
West Virginia University

Timothy E. Long
Marshall University

HHS Public Access

Author manuscript

Eur J Med Chem. Author manuscript; available in PMC 2019 January 01.

Published in final edited form as:

Eur J Med Chem. 2018 January 01; 143: 1185–1195. doi:10.1016/j.ejmech.2017.10.018.

Allicin-inspired pyridyl disulfides as antimicrobial agents for multidrug-resistant *Staphylococcus aureus*

Jordan G. Sheppard[a], **Jeremy P. McAleer**[a], **Pushkar Saralkar**[b], **Werner J. Geldenhuys**[b], and **Timothy E. Long**[a,c,*]

[a]Department of Pharmaceutical Science and Research, School of Pharmacy, Marshall University, Huntington, WV, USA

[b]Department of Pharmaceutical Sciences, School of Pharmacy, West Virginia University, Morgantown, WV, USA

[c]Department of Biomedical Sciences, Joan C. Edwards School of Medicine, Marshall University, Huntington, WV, USA

Abstract

A chemical library comprised of nineteen synthesized pyridyl disulfides that emulate the chemical reactivity of allicin (garlic) was evaluated for antimicrobial activity against a panel of pathogenic bacteria. Gram-positive species including vancomycin-intermediate and vancomycin-resistant *Staphylococcus aureus* (VISA, VRSA) demonstrated the highest level of susceptibility toward analogs with *S*-alkyl chains of 7–9 carbons in length. Further biological studies revealed that the disulfides display synergy with vancomycin against VRSA, cause dispersal of *S. aureus* biofilms, exhibit low cytotoxicity, and decelerate *S. aureus* metabolism. In final analysis, pyridyl disulfides represent a novel class of mechanism-based antibacterial agents that have a potential application as antibiotic adjuvants in combination therapy of *S. aureus* infections with reduced vancomycin susceptibility.

Keywords

Antibiotics; Disulfides; Narrow-spectrum; *Staphylococcus aureus*; Allicin; VRSA; MRSA; VISA

1. Introduction

Staphylococcus aureus is a bacterial pathogen of great clinical significance to public health [1]. Antibiotic-resistant forms including methicillin (MRSA), vancomycin-intermediate (VISA), and vancomycin-resistant (VRSA) variants are associated with invasive diseases in healthcare settings [2]. Multidrug-resistant (MDR) MRSA possessing resistance factors for three or more antibiotic classes are further implicated in high rates of antimicrobial treatment failures and chronic infections [1,2]. Consequentially, long-course treatment with first-line vancomycin (VAN) has led to the emergence of VISA and VRSA as impending and

*Corresponding author. Department of Pharmaceutical Science and Research, School of Pharmacy, Marshall University, Huntington, WV, USA. longt@marshall.edu (T.E. Long).

formable threats to public health [3]. Alternative antibiotics and treatment strategies therefore need to be developed to contend with these superbug infections.

Allicin is a natural thiosulfinate in garlic (*Allium sativum*) that has been investigated for an extensive range of medicinal applications including the treatment of bacterial infections [4]. Select Gram-positive pathogens including MRSA and *Bacillus anthracis* (anthrax) exhibit susceptibility to allicin at clinically-relevant minimum inhibitory concentrations (MICs) [5]. In addition, synergism with VAN has been reported for VAN-resistant *Enterococcus* (VRE) [6]. By chemical nature, allicin is electrophilic (δ+) and reacts with thiophilic, sulfhydryl-baring molecules such as cysteine, glutathione (GSH) and coenzyme A (CoASH) [7]. Multiple mechanisms have been proposed for the antibacterial action of allicin [4]. Each mutually involves a thiol-disulfide exchange reaction between the *S*-allyl constituent of allicin and the terminal thiol of an intracellular metabolite, coenzymes, or enzyme [4]. Inhibition of fatty acid biosynthesis is thought to be a primary mechanism of growth inhibition in bacteria [8]. Despite exhibiting antimicrobial properties against *S. aureus*, the chemical and thermal instability of allicin [9] has led to efforts to identify analogs for therapeutic development.

Pyridyl disulfides (**1**, PySSRs) are electrophilic reagents in the synthesis of asymmetric (mixed) disulfides that mimic the chemical reactivity of allicin (Fig. 1) [10]. At physiological pH, protonation of the pyridyl ring increases reactivity with thiophilic substances to accelerate the thiol-disulfide exchange reaction. With a reaction profile reminiscent of allicin, we embarked on an exploratory investigation to define the antibacterial activity of the mechanism-based PySSRs as antibacterial agents. In this article, the structure activity relationship (SAR) and pharmacodynamic properties of *S*-(alkylthio)-2-pyridine disulfides are reported.

2. Results and discussion

2.1. Chemistry

2.1.1. Synthesis of S-(alkylthio)-2-pyridine disulfides—For the study, a focused chemical library consisting of nineteen PySSR members **1a–s** (Scheme 1) derived from linear and branched thiols was prepared using classical organic chemistry. With exception of *S*-(methylthio) analog **1a**, the compounds were synthesized by a thiol-disulfide exchange reaction from commercially available 2′2-dipyridyl disulfide and each respective thiol in MeOH [10]. Unlike synthetic allicin [9,11], pyridyl disulfides **1b–s** were stable at r.t. following chromatographic purification. The only library member with which significant decomposition occurred after isolation was the *S*-methyl analog **1a**.

2.2. Biological studies

2.2.1. Antibacterial spectrum of activity—Preliminary antibacterial testing was performed by the disc diffusion (Kirby-Bauer) assay [12] using VAN and cefotaxime as comparators. The compounds were evaluated at equimolar concentrations of 10 μM in DMSO against a ten species panel that included five *S. aureus* variants. The disulfides exhibited narrow spectrum activity against Gram-positive bacteria including MDR *S. aureus*

(Table S1). Only Gram-negative *A. baumannii*, *E. coli*, and *E. cloacae* were weakly or partially inhibited by short chain analogs **1a–f**. Significant growth inhibition was indiscriminate for the majority of the PySSR analogs against *B. anthracis* and *S. epidermidis*. Conversely, there was a striking correlation between the *S*-alkyl chain length and zone diameter for *S. aureus*. Unbranched analogs with chain lengths of 5–9 carbons (**1e–i**) exhibiting the highest degree of growth inhibition were carried forward for MIC susceptibility testing. Synergism with VAN was also observed in the form of a bridging effect between the neighboring zone of disulfide **1h** (Fig. 2) and isobologram analysis was performed by the checkerboard titration assay.

2.2.2. Anti-MRSA activity—Susceptibility testing by the broth microdilution assay [12] indicated that PySSR derivatives **1g–i** of 7–9 carbon chains in length were the most effective growth inhibitors of planktonic *S. aureus* (Table 1). The MIC range against a panel comprised of six *S. aureus* variants was 1.56–25 μM (0.8–6.8 μg/mL) compared to 0.39 to >50 μM (1.2–>150 μg/mL) for VAN. Reduced susceptibility was noted for linezolid-resistant *S. aureus* (LRSA) and heterogeneous VISA (hVISA), but not for VISA and VanA-type VRSA [13] for disulfides **1g** and **1h**. Additional tests revealed that the disulfides disrupt *S. aureus* biofilms and exhibited a bacteriostatic profile with MBC:MIC ratios >4, a metric used to delineate bacteriostatic agents [14]. By contrast, VAN with a MBC:MIC ≤2 was confirmed to be bactericidal. In the biofilm reduction (dispersal) assay [15], preformed *S. aureus* biofilms were treated with 1–5× MIC of disulfide **1h** for 20 h and their densities were quantified by crystal violet (CV) staining. Fig. 3 shows that disulfide **1h** disrupted staphylococcal biofilms in a dose-dependent manner comparable to VAN.

Susceptibility testing was expanded to include additional clinical isolates of VISA and VRSA. The MIC_{90s} for both variants was 12.5 μM for PySSRs **1g–i** (Table 2). The compounds notably retained their antibacterial effects against the majority of the VanA-type VRSA strains. Accordingly, synergy testing was performed by isobologram analysis using the classical checkerboard titration assay [16] in 96 well plate format to establish whether the disulfides are able to lower the MIC of VAN in VRSA. In combination with 6.25 μM **1h**, susceptibility to VAN increased to MIC 1.56 μM from >50 μM (Fig. 4). The ΣFIC calculated from the MICs for each of the five lowest **1h**–VAN combinations equated to ≤0.5, a metric used to define synergism [17].

2.2.3. Resistance development studies—Development of antibiotic resistance in *S. aureus* is a frequent cause of treatment failure [2,3]. To compare the rates of resistance development in three variants of *S. aureus* (hVISA, VISA, and VRSA) to disulfide **1h**, a serial passage study was performed to monitor the changes in susceptibility in cultures treated with 0.5× MIC of antibiotic for 20 h. Fig 5 shows that between passages 3 and 4, hVISA followed by VRSA and VISA exhibited decreased susceptibility to the disulfide. Between passages 5 and 7, the MIC of each test strain increased again by twofold or greater. Most notable was the resistance development in hVISA from 12.5 μM to >50 μM indicating that a subpopulation of resistant clones predominated after seven passages [18]. During the course of the study, we also monitored alterations in the MICs when disulfide **1h** was combined with an equimolar amount of VAN. After seven passages, the only observed

change was a twofold increase in the MIC with VRSA and hVISA between passages 2 and 4 (Fig. 5).

2.2.4. Effect of blood components studies—Due to their electrophilic and lipophilic properties, it was anticipated that the antibacterial activity of PySSRs may be altered by one or more components in bloods. Table 3 shows that media supplemented with GSH and 5–10% fetal bovine serum (FBS) increased the MICs of disulfides **1g–i**, which was attributed to cleavage of the disulfide bond by GSH and serum protein binding, respectively. By comparison, the MICs of OXA and VAN were not affected by the additives. We similarly found that GSH and serum decreases the anti-MSSA activity of disulfiram (Antabuse™), a FDA-approved disulfide drug for the treatment of chronic alcoholism [19]. Based on these data, we concluded that *in vivo* dosing of PySSRs would have to compensate for blood components in a manner similar to disulfiram and other disulfide drugs (e.g., prosultiamine).

2.2.5. Cytotoxicity studies—Disulfides **1e–i** were evaluated for cytotoxicity using human breast MDA-MB-231 and liver HepG2 carcinoma cell lines. Fig. 6 shows that the half-maximal inhibitory concentrations (IC_{50s}) are greater than the MIC_{90s} of 12.5 μM for VISA and VRSA. For disulfide **1h**, the IC_{50s} were 74.9 and ≥ 100 μM for the respective cell lines. The attenuated cytotoxic activity was attributed to the GSH-rich content in mammalian cells. The thiophilic tripeptide has been shown to cancel out the antimicrobial activity of allicin in bacteria through thiol-disulfide exchange [7] and it is believed that GSH inactivates the PySSRs in mammalian cells. To this end, the Gram-positive species that exhibit susceptibility to the disulfides **1e–i** have low intracellular GSH levels and alternatively use CoASH and bacillithiol in thiol-redox buffering [20]. A similar rationale is proposed for the lack of antimicrobial activity in Gram-negative bacteria that contain high levels of cytosolic GSH to maintain redox homeostasis [20,21].

2.2.6. Viability studies—To further examine the effects of PySSR **1h** on bacteria viability, we performed a series of growth and metabolic studies on *S. aureus*. Fig. 7A shows that treatment with 1–2× MIC suppressed growth over a 20 h period while exposure to 0.25 and 0.5× MIC of **1h** delayed proliferation for 10 and 15 h, respectively. Likewise, treatment with 1 and 4× MIC attenuated the growth rate with little change in CFU numbers, which again suggested that the PySSRs are bacteriostatic in nature (Fig. 7B). In a follow-up study performed in HBSS with phenol red pH indicator, disulfide **1h** was found to decelerate the metabolism of glucose to organic acids in a manner comparable to triclosan at a bacteriostatic test concentration (data not shown).

Bacteriostatic antibiotics have been previously shown to decelerate respiration and lower the cellular metabolic state in *S. aureus* [22]. By contrast, bactericidal agents were found to accelerate respiration and metabolism [23]. To further decipher the effect on metabolism, the C_{12}-resazurin viability assay was used to detect for alterations in the redox activity of *S. aureus* treated with PySSR **1h**. Fig. 8A shows that the disulfide decelerates metabolism in a similar manner to the positive control NaF. Although these results were again consistent with the bacteriostatic assessment, we further probed the effects on cell viability using the LIVE/DEAD *Bac*Light™ assay. In the experiment, membrane permeability (damage) as a measure of cell viability is determined by comparing the green to red fluorescence ratio

(λ_{em} 535/595 nm) of bacteria co-labeled with SYTO™ 9 and propidium iodide. Fig. 8B shows a negligible difference in membrane integrity between untreated and PySSR **1h** treatment groups. Conversely, a significant increase in membrane permeability was observed for the pore-forming antibiotic nisin.

2.2.7. Plasma membrane studies—With compelling data that revealed the disulfides to be bacteriostatic agents that decelerate metabolism, we evaluated the effect of PySSRs on electron transport through differential measurements of the membrane potential. In the experiment, *S. aureus* was treated with either PySSR **1h**, de-coupler CCCP (positive control), or ciprofloxacin (negative control). The cells were then labeled with $DiOC_2(3)$ and analyzed by flow cytometry at λ_{ex} 488 nm. At 15 and 30 min intervals, the disulfide was found to dissipate the membrane potential ($\Delta\Psi$) in both a time- and concentration-dependent manner (Fig. 9). Rapid depolarization was observed within 15 min of treatment with 3–30 μM of the test drug. Between 15 and 30 min, moderate increases in membrane potentials were observed for the groups treated with **1h (**15–30 μM), but not the CCCP control.

2.2.8. Cellular redox studies—The antagonistic effects on the membrane potential and metabolism suggested that PySSRs could evoke a shift in the intracellular redox state. Within this context, *S. aureus* employs CoASH with bacillithiol in place of GSH as the major thiol involved in redox homeostasis [20,24]. Previous studies have shown that allicin reduces cellular thiol levels and alters both the metabolic and redox states of cells [25,26]. Based on these previous findings, we postulated that PySSR **1h** mimics the antibacterial action of allicin by disrupting metabolism and thiol-redox buffering in *S. aureus*. To this end, growth inhibition by the disulfides was partly attributed to alterations in cytosolic thiol levels and the cellular redox state. To first establish whether PySSRs could decrease thiol levels through–SR exchange (Fig. 1), PyS*SR* **1h** was incubated with equimolar CoASH and mass spectroscopy was used to verify CoS*SR* formation (Fig. 10A).

With confirmation of a thiol-disulfide exchange with CoASH, it was believed that perturbations in the cellular redox state is partly responsible for the antimicrobial effects of PySSRs. We explored this premise by labeling treated *S. aureus* cells with the oxidant-reactive probes nitroblue tetrazolium (NBT) [27] and 2′,7′-dicholorodihydrofluorescin-diacetate (DCFH-DA) [28]. Triclosan was included in the experiments as a O_2^- generating positive control [29]. In the NBT assay, oxidation of the chromogenic probe was detected within 1 h of treatment with disulfide **1h** and triclosan in *S. aureus* (Fig. 10B). Increased formation of oxidized DCFH [30] was also observed for PySSR **1h**, but at a lower rate compared to triclosan (Fig. 10C). It should be noted that although these experiments revealed accelerated oxidation rates of the NBT and DCFH-DA probes, further studies are needed to establish whether the inhibitory effects of disulfide-based antibacterial drugs can be attributed to a shift in the cellular redox state in *S. aureus* [31].

3. Conclusions

S. aureus is an invasive, toxigenic pathogen that can inflict disease on every tissue, organ, and system in the human body [1,2]. MDR strains with reduced glycopeptide susceptibility are an emerging healthcare threat and new treatment strategies will be needed for patients

with these resistant infections [3]. Thio-sulfinates such as allicin represent a unique mechanistic drug class whose activity spectrum is largely confined to Gram-positive species that includes *S. aureus* [5]. In this report, we have identified pyridyl disulfides as stable alternatives to allicin with a similar narrow spectrum profile. All twenty-five strains of *S. aureus* used in the study exhibited the highest susceptibility to PySSR derivatives bound with linear *S*-alkyl chains of 7–9 carbons in length. Quality control MRSA 43300 and VanA-type VRSA were equally susceptible to the disulfides; however, LRSA and hVISA were less sensitive for undetermined reasons. The latter was also found to have a higher rate of resistance development compared to VISA and VRSA variants (Fig. 5). Our serial passage experiment further revealed a lower rate of resistance selection when disulfide **1h** was combined with equimolar VAN versus the disulfide alone.

In addition, the 8 carbon chain derivative **1h** was identified in the disc diffusion assay as having synergy with VAN through observation of a bridging effect between the adjacent zones (Fig. 2) and further testing by isobologram analysis corroborated this relationship (Fig. 4). Although a basis for the synergistic relationship in VRSA could not be definitively established, we initiated preliminary investigative work to understand how PySSRs function as a growth inhibitor of *S. aureus*. Their bacteriostatic nature suggests that the pharmacodynamic effects are due to deceleration in cellular metabolism; however, PySSRs may also evoke a shift in the redox state that triggers perturbations of cell processes involved in growth [22]. Accordingly, an increase in the cellular oxidation state of bacteria has been shown to alter metabolic activity (e.g., respiration) [22] and gene expression [32]. Redox regulation in *S. aureus* is coordinated by low molecular weight thiols CoASH and bacillithiol rather than GSH [20]. Increased intracellular oxidant levels results in a decrease of the thiol:disulfide redox ratio and increased *S*-bacillithiolation of proteins, which is believed to protect against cytotoxic effects in *S. aureus* [24,33].

Within this context, mass spectroscopy revealed that thiol-disulfide exchange occurs between electrophilic PySSRs and thiophilic CoASH (Fig. 10A). Based on this finding, we hypothesize that the antimicrobial action of PySSR is partially attributed to pro-oxidant effects in *S. aureus* due to the thiol-disulfide exchange reactions in the cell. Increased oxidation of NBT and DCFH-DA was observed with disulfide treatment (Fig. 10B and C); however, further studies are needed to deduce the effects on the cellular redox state [31]. Another key finding of the investigation is that PySSR **1h** decreases the membrane potential (Fig. 9) without damaging the plasma membrane (Fig. 8B). Based on these data, it is believed that the deceleration of metabolism by bacteriostatic PySSRs curbs respiration, de-energizing the cell membrane [22].

In final analysis, our data shows that PySSRs are bacteriostatic agents in Gram-positive pathogens including MDR variants of *S. aureus*. The disulfides possess a narrow activity spectrum and are thought to function as pro-oxidants in a manner reminiscent of allicin [4,25]. Our studies found that the mechanism-based PySSRs suppress metabolism presumably through interactions with thiophilic metabolites, coenzymes, and/or enzymes. These data further suggest that PySSRs have more than one mechanism of action responsible for the growth inhibition in *S. aureus*. Concomitantly, the onset of resistance would expect to be lower for an antibacterial agent that inhibits multiple cell processes;

however, our serial passage experiments revealed the occurrence of resistance selection in *S. aureus* treated with 0.5× MIC PySSR **1h**. With these findings, it is believed that the application of allicin-like drugs in antimicrobial therapy is limited to use as combination treatments for Gram-positive bacterial infections with reduced VAN susceptibility. Future investigations will focus on analyzing the potential place in therapy of disulfide-based drugs as adjuvant antibiotics for MDR *S. aureus* infections.

4. Materials and methods

4.1. Chemistry

Chemicals were purchased from commercial sources and used as received. Products were purified by flash chromatography on 60–100 mesh silica and visualized by UV on TLC plates (silica gel 60 F_{254}). ^{1}H and ^{13}C NMRs were recorded on a 400 MHz NMR and referenced to residual $CDCl_3$. Abbreviations used in the description of resonances are as follow: s (singlet); bs (broad singlet); d (doublet); t (triplet); q (quartet); qnt (quintet); m (multiplet); dt (doublet of triplets); ddd (doublet of doublets of doublets).

4.1.1. Synthesis of pyridyl disulfides 1; general procedure—Asymmetric *S*-(alkylthio)-2-pyridine disulfides were prepared by a modified procedure of previously reported methods [10]. To a stirring solution of 2′2-dipyridyl disulfide (0.75 mmol) and AcOH (25 μL) in 9 mL of MeOH was added the corresponding thiol (0.75 mmol) in 1 mL of MeOH at r.t. The mixture was stirred for 2–6 h and concentrated *in vacuo*. Flash silica gel chromatography with 0–25% EtOAc in hexanes afforded the pure asymmetric disulfides **1b–s** as pale oils [10]. The *S*-methyl analog **1a** was prepared from 2-mercaptopyridine (0.75 mmol) and *S*-methyl methanethiosulfonate (0.75 mmol) in 10 mL of MeOH. After stirring for 2 h at r.t., the solvent was evaporated and the product was isolated as a pale oil by flash silica gel chromatography with 3:1 hexanes:EtOAc. The spectroscopic data for disulfides **1e–i** are provided.

4.1.1.1. S-(pentylthio)-2-pyridine (1e): ^{1}H NMR (400 MHz, $CDCl_3$) δ 8.45 (ddd, J = 4.9, 1.8, 0.9 Hz, 1H), 7.73 (dt, J = 8.1, 1.0 Hz, 1H), 7.69–7.59 (m, 1H), 7.07 (ddd, J = 7.4, 4.8, 1.1 Hz, 1H), 2.83–2.75 (m, 2H), 1.69 (q, J = 7.4 Hz, 2H), 1.43–1.24 (m, 5H), 0.88 (t, J = 7.2 Hz, 3H); ^{13}C NMR (101 MHz, $CDCl_3$) δ 160.7, 149.5, 136.9, 120.5, 119.5, 39.2, 30.7, 28.6, 22.3, 13.92; ESI–MS: *m/z* 214.1 $[M+H]^+$

4.1.1.2. S-(hexylthio)-2-pyridine (1f): ^{1}H NMR (400 MHz, $CDCl_3$) δ 8.45 (ddd, J = 4.9, 1.9, 0.9 Hz, 1H), 7.73 (dt, J = 8.1, 1.1 Hz, 1H), 7.63 (ddd, J = 8.1, 7.4, 1.8 Hz, 1H), 7.07 (ddd, J = 7.3, 4.8, 1.1 Hz, 1H), 2.83–2.75 (m, 2H), 1.75–1.61 (m, 1H), 1.44–1.28 (m, 4H), 1.32–1.21 (m, 6H), 0.87 (t, J = 7.5 Hz, 2H).; ^{13}C NMR (101 MHz, $CDCl_3$) δ 160.7, 149.5, 136.9, 120.4, 119.5, 39, 31.4, 28.9, 28.2, 22.5, 14; ESI–MS: *m/z* 228.2 $[M+H]^+$.

4.1.1.3. S-(heptylthio)-2-pyridine (1g): ^{1}H NMR (400 MHz, $CDCl_3$) δ 8.45 (ddd, J = 4.8, 1.8, 0.9 Hz, 1H), 7.73 (dt, J = 8.1, 1.0 Hz, 1H), 7.63 (ddd, J = 8.1, 7.4, 1.8 Hz, 1H), 7.07 (ddd, J = 7.4, 4.8, 1.1 Hz, 1H), 2.83–2.74 (m, 2H), 1.68 (q, J = 7.5 Hz, 2H), 1.43–1.28 (m, 3H), 1.25–1.40 (m, 8H), 0.91–0.82 (m, 3H).; ^{13}C NMR (101 MHz, $CDCl_3$) δ 160.7, 149.5, 136.9, 120.4, 119.5, 39, 31.7, 28.9, 28.4, 22.6, 14.1; ESI–MS: *m/z* 242.2 $[M+H]^+$.

4.1.1.4. S-(octylthio)-2-pyridine (1h): ^{1}H NMR (400 MHz, $CDCl_3$) δ 8.44 (ddd, J = 4.8, 1.8, 0.9 Hz, 1H), 7.73 (dt, J = 8.1, 1.0 Hz, 1H), 7.63 (ddd, J = 8.1, 7.4, 1.9 Hz, 1H), 7.06 (ddd, J = 7.4, 4.8, 1.1 Hz, 1H), 2.83–2.74 (m, 2H), 1.68 (qnt, J = 7.3 Hz, 2H), 1.43–1.17 (m, 10H), 0.92–0.81 (m, 3H); ^{13}C NMR (101 MHz, $CDCl_3$) δ 160.7, 149.5, 136.9, 120.5,119.5, 39, 31.8, 29.2 (2), 29, 28.5, 22.7,14.1; ESI–MS: *m/z* 256.2 $[M+H]^+$.

4.1.1.5. S-(nonylthio)-2-pyridine (1i): ^{1}H NMR (400 MHz, $CDCl_3$) δ 8.44 (ddd, J = 4.8, 1.8, 0.9 Hz, 1H), 7.73 (dt, J = 8.1, 1.0 Hz, 1H), 7.63 (ddd, J = 8.1, 7.4, 1.9 Hz, 1H), 7.06 (ddd, J = 7.4, 4.8, 1.1 Hz, 1H), 2.85–2.67 (m, 2H), 1.68 (qnt, J = 7.3 Hz, 2H), 1.44–1.16 (m, 10H), 0.91–0.84 (m, 3H); ^{13}C NMR (101 MHz, $CDCl_3$) δ 160.7, 149.5, 136.9, 120.4, 119.5, 38, 31.8, 29.4, 29.2, 29.2, 28.9, 28.5, 22.6, 14.1; ESI–MS: *m/z* 270.2 $[M+H]^+$

4.2. Biological studies

Bacteria used in the study are listed in Tables S1 and S2 in the supplemental material. Bacteria were initially grown on Mueller-Hinton agar (MHA) from freezer stocks stored at −80 °C. Tryptic soy broth (TSB) and Luria-Bertani (LB) broth were used to grow starter cultures from single colonies for testing. Mammalian cell lines used in the study were propagated in Dulbecco's Modified Eagle's medium (DMEM) containing 10% fetal bovine serum (FBS) from freezer stocks stored at −150 °C.

4.2.1. MIC and MBC determination—Minimal inhibitory concentrations (MICs) were determined by the broth microdilution method in 96-well flat bottom microplates [12]. A 0.5 McFarland standardized suspension prepared from an overnight culture was diluted to 1:100 in cation-adjusted Mueller Hinton broth (CAMHB) and treated with serial dilutions of test agents for 20 h at 37 °C. The lowest drug concentration that gave inhibition of visual growth was recorded as the MIC. The MIC_{50} and MIC_{90} values were defined as the lowest concentration by which 50 and 90%, respectively, of the strains were inhibited by the test agent. The minimal bactericidal concentrations (MBCs) were determined by spotting 5 μL aliquots from each well on agar media. Following overnight incubation, the lowest concentration to inhibit visual growth was recorded as the MBC.

4.2.2. Biofilm reduction assay—To assess for biofilm dispersal, biofilms were grown in a flat bottom 96-well microplate (Corning, Inc.) using 200 μL of a 1.5–2.0 × 10^5 inoculum of *S. aureus* 25293 in CAMHB [15]. After 30 h incubation at 37 °C, the media was removed by aspiration, the wells were washed with PBS, and the residual biofilms were treated with 1–5× MIC of test agent in 100 μL of CAMHB. Following 20 h incubation at 37 °C, the media was removed and the biofilms were treated for 0.5 h with 200 μL of aqueous 0.1% crystal violet. The staining solution was then discarded, the wells were washed with PBS, and 200 μL of 30% acetic acid (vol/vol) was added to solubilize the dye retained by the biofilms. Biofilm dispersal was assessed by comparing the optical absorption (OD_{595}) of the acetic acid solutions from the treated vs. untreated wells.

4.2.3. Synergy studies—Isobologram analysis of PySSR-VAN treatment combinations was performed by the classical checkerboard titration assay [16]. Briefly, a 0.5 McFarland suspension of VRSA HIP14300 was diluted to 1:100 in CAMHB and 50 μL was used to

inoculate a 96-well plate containing twofold serial dilutions of PySSR and VAN in 50 μL CAMHB. The plates were then sealed with adhesive film and incubated for 20 h at 37 °C. Growth inhibition was visualized by MTT staining using DMSO to solubilize the formazan product. The fractional inhibition (FIC) index was determined by the ratio of MIC of the combination treatment to the MIC of PySSR **1h** or VAN alone. The ΣFIC ($FIC_{\mathbf{1h}} + FIC_{VAN}$) was interpreted according to the standard metrics: synergy ≤ 0.5; indifferent 0.5 < to ≤ 4; antagonism > 4 [17].

4.2.4. Growth studies—An overnight inoculum of *S. aureus* 25293 was grown to an OD_{600} of 0.1 and treated with 0, 0.25, 0.5, 1, and 2× MIC of test agents in a 96-well microplate. The plate was incubated at 37 °C in a Multiskan GO microplate reader (Thermo Fisher Scientific, Inc.) and the OD_{600} was measured at 1 h intervals following 30 s agitation. The results were plotted using GraphPad Prism. Time-kill studies were performed using a 1:100 dilution of 0.5 McFarland suspension of *S. aureus* 25293 treated with 0,1, and 4× MIC of test agent [34]. At time points 0, 1, 2, and 4 h, 10 μL samples were serially diluted in PBS and streaked onto MHA plates to enumerate the bacteria. Colony forming units (CFUs) were totaled after 30 h incubation and the data was plotted using GraphPad Prism.

4.2.5. Resistance studies—The serial passage assay [35] to determine resistance development was performed using hVISA Mu3, VISA AR-217, and VRSA AIS 1000505 treated with 0.5× MIC of PySSR **1h** ± equimolar VAN. A 0.5 McFarland standardized suspension of each 0.5× MIC culture was diluted to 1:100 in CAMHB and treated with serial dilutions of the test agents. Following incubation for 20 h at 37 °C, the MICs were determined by visual inspection for each passage.

4.2.6. Cytotoxicity studies—The MTT assay was used to assess cellular viability by measuring the NAD(P)H-dependent cellular oxidoreductase enzyme activity. The yellow dye (3-(4,5-dimethylthiazol-2-yl)-2,5-diphenyltetrazolium bromide) is converted to an insoluble blue formazan. Human breast adenocarcinoma cells MDA-MB-231 and human liver carcinoma cells HepG2 were seeded at 5000 cells per well in a 96-well plate, and allowed to adhere overnight. The next day, 0.001, 0.01, 0.1, 10, and 100 μM of test agents were added to the cells and incubated for 72 h. At the end of the experiment, the media was removed and MTT dye at 1 mg/mL in PBS pH 7.4 was added to each well and incubated for 2 h. The MTT solution was then removed and pure DMSO added to each well and incubated in orbital shaker for 30 min at 37 °C until the crystals were dissolved. The absorbance was measured at OD_{570} in a BioTek Synergy H plate reader (BioTek Instruments, Inc.).

4.2.7. Viability studies—The LIVE/DEAD *Bac*Light™ assay (Molecular Probes, Inc.) to determine cell viability and membrane damage was performed on an overnight innocuum of *S. aureus* 25293 grown to an OD_{600} of 0.4 in LB broth. The cells were harvested by centrifugation (10,000 × *g*, 10 min, 4 °C), washed twice with PBS and resuspended in 100 mM phosphate buffer (KH_2PO_4/K_2HPO_4, pH 7.0) supplemented with 5 mM $MgSO_4$. The bacteria were then energized with glucose (20 mM final concentration) for 10 min at 37 °C and treated with 1 or 5× MIC of test agent. Vehicle (DMSO; 5%) and 25 μg/mL nisin, a pore-forming antibiotic, were used as controls [36]. After 5 min incubation, 100 μL samples

were combined with 100 μL of a 2×*Bac*Light™ staining reagent in a black flat bottom 96-well microplate (Corning, Inc.) and mixed. The plate was covered and allow to stand at r.t. in the absence of light. After 15 min, the fluorescence emission of green (λ_{ex} 485 nm, λ_{em} 535 nm) to red (λ_{ex} 485 nm, λ_{em} 595 nm) ratio was measured on a Filter Max F3 fluorescent plate reader (Molecular Devices, Inc.). Membrane permeability (damage) as a measure of cell viability was determined by comparing the green to red fluorescence ratio (λ_{em} 535/595 nm) between treatment groups.

4.2.8. Metabolic activity assay—The Vybrant™Cell Metabolic assay (Invitrogen, Inc.) to measure metabolic (redox) activity of viable bacterial cells was performed on an overnight innocuum of *S. aureus* 25293 grown to an OD_{600} of 0.4 in LB broth. Cells were treated with 0.25, 0.5, or 1× MIC of test agent. Vehicle (DMSO; 5%) and NaF (5 mM), an inhibitor of glycolysis [36], were used as controls. After 15 min at 37 °C, aliquots of 200 μL were combined with 5 μM C_{12}-resazurin in a black flat bottom 96-well microplate and incubated in the dark for 15 min. Metabolic activity was measured by the fluorescence intensity of the reduced metabolite C_{12}-resorufin (λ_{ex} 550 nm, λ_{em} 595 nm).

4.2.9. Glucose metabolism—Phenol red pH indicator was used to detect for glucose metabolism as a measure of increased acidity of the medium. A 90 μL innocuum of a OD_{600} 1.0 suspension of *S. aureus* 25293 in Hank's buffered salt solution (HBSS) was combined with 150 μL of 70 μM phenol red in water and 10 μL of either 2 mM disulfide, triclosan, vehicle (DMSO), or water in a 96-well plate. The plate was incubated at 37 °C in a Multiskan GO microplate reader for 15 h with OD_{560} readings at 0.5 h intervals.

4.2.10. Membrane potential assay—The *Bac*Light™ Bacterial Membrane Potential kit (Molecular Probes, Inc.) was used to detect for drug-induced alterations in the proton gradient of *S. aureus*. An overnight culture was diluted 1:100 in LB, incubated at 37 °C with shaking for 2 h, and used to make a final 1:200 dilution for the experiment. Cells were treated with PySSR **1h** (3–30 μM), vehicle, (DMSO; 2%) or the respiratory decoupler carbonyl cyanide *m*-chlorophenyl hydrazone (CCCP) and incubated at 37 °C with shaking. After 15 and 30 min, 200 μL samples were transferred to a fresh tube containing 2 μL of the fluorescent membrane potential indicator dye $DiOC_2(3)$. $DiOC_2(3)$ emits green fluorescence in all cells, but larger membrane potentials cause a shift towards red emission due to self-association of the dye at higher cytosolic concentrations [37]. After staining for 20 min, bacteria were analyzed on a BD Biosciences FACSAria with the following parameters: λ_{ex} 488 nm, green fluorescence filter 530/30 and red fluorescence filter 585/42. The resulting data was processed using FlowJo v10.1 software (FlowJo, LLC).

4.2.11. NBT and DCFH-HA assays—The colorimetric nitroblue tetrazolium (NBT) assay [27] to detect for alterations in intracellular oxidation rates was performed using a OD_{600} 1.5 suspension of *S. aureus* 25293 in HBSS. A 80 μL innocuum was combined with 150 μL aqueous solution of 1 mg/mL NBT and 10 μL of either 2 mM PySSR **1h**, triclosan, vehicle (DMSO), or water in a 96-well microplate and incubated with shaking for 1 h at 37 °C. The reaction was stopped with 10 μL 0.1 M HCl, the plate was centrifuged at 1500 × *g* for 10 min at 0 °C, and the supernatant was removed. The pellets were then treated with 25

μL of DMSO, 10 μL 2 N KOH, and 50 μL of HBSS to solubilize the formazan product. Intracellular oxidant species generation was measured by the intensity of blue coloration at OD_{560}.

The fluorometric 2′,7′–dichlorofluorescin diacetate (DCFH-HA) assay [28] was similarly performed using a OD_{600} 1.5 suspension of *S. aureus* 25293 in HBSS. To 80 μL of inoculums in a black flat bottom 96-well microplate was added 5 μL of either 2 or 10 mM PySSR **1h**, 10 mM triclosan, vehicle (DMSO), or water followed by 15 μL of 100 μM DCFH-HA in DMSO. Intracellular oxidation of deacylated DCFH was measured by the intensity of fluorescence (λ_{ex} 485 nm, λ_{em} 535 nm).

4.3. Statistical analyses

Data are presented as ± standard error of the mean (SEM). Statistical significance was assessed by analysis of variance (ANOVA) with Tukey's posttest for multiple comparisons using Prism 5.0 (GraphPad Software, Inc) software. *P* values of < 0.05 were considered significant.

Supplementary Material

Refer to Web version on PubMed Central for supplementary material.

Acknowledgments

This research was supported by the Marshall University School of Pharmacy FRS Grant Program. The authors also thank Marshall University Department of Chemistry for use of the NMR facility and Dr. Mohammad F. Hossain for mass spectroscopy analyses. Bacterial strains were acquired from the American Type Culture Collection, FDA-CDC Antimicrobial Resistance Isolate Bank, and the Network on Antimicrobial Resistance in *Staphylococcus aureus* (NARSA) for distribution by BEI Resources, NIAID, NIH.

References

1. Boucher HW, Corey GR. Epidemiology of methicillin-resistant *Staphylococcus aureus*. Clin Infect Dis. 2008; 46:S344–S349. [PubMed: 18462089]
2. Gould IM, David MZ, Esposito S, Garau J, Lina G, Mazzei T, Peters G. New insights into methicillin-resistant Staphylococcus aureus (MRSA) pathogenesis, treatment and resistance. Int J Antimicrob Agents. 2012; 39:96–104. [PubMed: 22196394]
3. Gould IM. Treatment of bacteremia: methicillin-resistant *Staphylococcus aureus* (MRSA) to vancomycin-resistant S. aureus (VRSA). Int J Antimicrob Agents. 2013; 42:S17–S21. [PubMed: 23664580]
4. Borlinghaus J, Albrecht F, Gruhlke MC, Nwachukwu ID, Slusarenko AJ. Allicin: chemistry and biological properties. Molecules. 2014; 19:12591–12618. [PubMed: 25153873]
5. Ankri S, Mirelman D. Antimicrobial properties of allicin from garlic. Microbes Infect. 1999; 1:125–129. [PubMed: 10594976]
6. Jonkers D, Sluimer J, Stobberingh E. Effect of garlic on vancomycin-resistant enterococci. Antimicrob Agents Chemother. 1999; 43:3045. [PubMed: 10651625]
7. Fujisawa H, Watanabe K, Suma K, Origuchi K, Matsufuji H, Seki T, Ariga T. Antibacterial potential of garlic-derived allicin and its cancellation by sulfhydryl compounds. Biosci Biotechnol Biochem. 2009; 73:1948–1955. [PubMed: 19734685]
8. Focke M, Feld A, Lichtenthaler K. Allicin, a naturally occurring antibiotic from garlic, specifically inhibits acetyl-CoA synthetase. FEBS Lett. 1990; 261:106–108. [PubMed: 1968399]

9. Fujisawa H, Suma K, Origuchi K, Kumagai H, Seki T, Ariga T. Biological and chemical stability of garlic-derived allicin. J Agric Food Chem. 2008; 56:4229–4235. [PubMed: 18489116]
10. Barton DHR, Hesse RH, O'Sullivan AC, Pechet MM. A new procedure for the conversion of thiols into reactive sulfenylating agents. J Org Chem. 1991; 56:6697–6702.
11. Sheppard JG, Long TE. Allicin-inspired thiolated fluoroquinolones as antibacterials against ESKAPE pathogens. Bioorg Med Chem Lett. 2016; 26:5545–5549. [PubMed: 27756563]
12. Jorgensen, JH., Turnidge, JD. Antibacterial susceptibility tests: dilution and disk diffusion methods. In: Murray, PR.Baron, EJ.Jorgensen, JH.Landry, ML., Pfaller, MA., editors. Manual of Clinical Microbiology. ASM Press; Washington, DC: 2007. p. 1152-1172.
13. Périchon B, Courvalin P. VanA-type vancomycin-resistant *Staphylococcus aureus*. Antimicrob Agents Chemother. 2009; 53:4580–4587. [PubMed: 19506057]
14. Pankey GA, Sabath LD. Clinical relevance of bacteriostatic versus bactericidal mechanisms of action in the treatment of Gram-positive bacterial infections. Clin Infect Dis. 2004; 38:864–870. [PubMed: 14999632]
15. Bauer J1, Siala W, Tulkens PM, Van Bambeke F. A combined pharmacodynamic quantitative and qualitative model reveals the potent activity of daptomycin and delafloxacin against Staphylococcus aureus biofilms. Antimicrob Agents Chemother. 2013; 57:2726–2737. [PubMed: 23571532]
16. Moody, JA. Synergism testing: broth microdilution checkboard and broth macrodilution methods. In: Isenberg, HD., editor. Clinical Procedures Handbook. ASM Press; Washington, DC: 1992. p. 5.18.1-5.18.28.
17. Odds FC. Synergy, antagonism, and what the chequerboard puts between them. J Antimicrob Chemother. 2003; 52:1. [PubMed: 12805255]
18. Howden BP, Davies JK, Johnson PD, Stinear TP, Grayson ML. Reduced vancomycin susceptibility in Staphylococcus aureus, including vancomycin-intermediate and heterogeneous vancomycin-intermediate strains: resistance mechanisms, laboratory detection, and clinical implications. Clin Microbiol Rev. 2010; 23:99–139. [PubMed: 20065327]
19. Long TE. Repurposing thiram and disulfiram as antibacterial agents for multi-drug resistant Staphylococcus aureus infections. Antimicrob Agents Chemother. 2017; 61:e00898–17. [PubMed: 28674046]
20. Loi VV, Rossius M, Antelmann H. Redox regulation by reversible protein *S*-thiolation in bacteria. Front Microbiol. 2015; 6:187. [PubMed: 25852656]
21. Fahey RC, Brown WC, Adams WB, Worsham MB. Occurrence of glutathione in bacteria. J Bacteriol. 1978; 133:1126–1129. [PubMed: 417060]
22. Lobritz MA, Belenky P, Porter CB, Gutierrez A, Yang JH, Schwarz EG, Dwyer DJ, Khalil AS, Collins JJ. Antibiotic efficacy is linked to bacterial cellular respiration. Proc Natl Acad Sci U S A. 2015; 112:8173–8180. [PubMed: 26100898]
23. Belenky P, Ye JD, Porter CB, Cohen NR, Lobritz MA, Ferrante T, Jain S, Korry BJ, Schwarz EG, Walker GC, Collins JJ. Bactericidal antibiotics induce toxic metabolic perturbations that lead to cellular damage. Cell Rep. 2015; 13:968–980. [PubMed: 26565910]
24. Chi BK, Roberts AA, Huyen TT, Bäsell K, Becher D, Albrecht D, Hamilton CJ, Antelmann H. S-bacillithiolation protects conserved and essential proteins against hypochlorite stress in firmicutes bacteria. Antioxid Redox Signal. 2013; 18:1273–1295. [PubMed: 22938038]
25. Müller A, Eller J, Albrecht F, Prochnow P, Kuhlmann K, Bandow JE, Slusarenko AJ, Leichert LI. Allicin induces thiol stress in bacteria through S-Allylmercapto modification of protein cysteines. J Biol Chem. 2016; 291:11477–11490. [PubMed: 27008862]
26. Gruhlke MC, Portz D, Stitz M, Anwar A, Schneider T, Jacob C, Schlaich NL, Slusarenko AJ. Allicin disrupts the cell's electrochemical potential and induces apoptosis in yeast. Free Radic Biol Med. 2010; 49:1916–1924. [PubMed: 20883774]
27. Albesa I, Becerra MC, Battán PC, Páez PL. Oxidative stress involved in the antibacterial action of different antibiotics. Biochem Biophys Res Commun. 2004; 317:605–609. [PubMed: 15063800]
28. Dridi B, Lupien A, Bergeron MG, Leprohon P, Ouellette M. Differences in antibiotic-induced oxidative stress responses between laboratory and clinical isolates of *Streptococcus pneumoniae*. Antimicrob Agents Chemother. 2015; 59:5420–5426. [PubMed: 26100702]

29. Kovacic, P., Somanathan, R. Triclosan (mechanism of bactericidal action and toxicity): metabolism, electron transfer and reactive oxygen species. In: Hepel, M., Andreescu, S., editors. Oxidative Stress: Diagnostics, Prevention, and Therapy, Vol. 2 ACS Symposium Series. American Chemical Society; Washington, DC: 2015. p. 237-244.

30. Dwyer DJ, Belenky PA, Yang JH, MacDonald IC, Martell JD, Takahashi N, Chan CT, Lobritz MA, Braff D, Schwarz EG, Ye JD, Pati M, Vercruysse M, Ralifo PS, Allison KR, Khalil AS, Ting AY, Walker GC, Collins JJ. Antibiotics induce redox-related physiological alterations as part of their lethality. Proc Natl Acad Sci U S A. 2014; 111:E2100–E2109. [PubMed: 24803433]

31. Liu Y, Imlay JA. Cell death from antibiotics without the involvement of reactive oxygen species. Science. 2013; 339:1210–1213. [PubMed: 23471409]

32. Chang W, Small DA, Toghrol F, Bentley WE. Global transcriptome analysis of *Staphylococcus aureus* response to hydrogen peroxide. J Bacteriol. 2006; 188:1648–1659. [PubMed: 16452450]

33. Posada AC, Kolar SL, Dusi RG, Francois P, Roberts AA, Hamilton CJ, Liu GY, Cheung A. Importance of bacillithiol in the oxidative stress response of *Staphylococcus aureus*. Infect Immun. 2014; 82:316–332. [PubMed: 24166956]

34. Verma, P. Methods for determining bactericidal activity and antimicrobial interactions: synergy testing, time-kill curves, and population analysis. In: Schwalbe, R.Steele-Moore, L., Goodwin, AC., editors. Antimicrobial Susceptibility Testing Protocols. CRC Press; Boca Raton, FL: 2007. p. 275-298.

35. Goldstein BP, Draghi DC, Sheehan DJ, Hogan P, Sahm DF. Bactericidal activity and resistance development profiling of dalbavancin. Antimicrob Agents Chemother. 2007; 1:1150–1154.

36. Swe PM, Cook GM, Tagg JR, Jack RW. Mode of action of dysgalacticin: a large heat-labile bacteriocin. J Antimicrob Chemother. 2009; 63:679–686. [PubMed: 19213799]

37. Novo D, Perlmutter NG, Hunt RH, Shapiro HM. Accurate flow cytometric membrane potential measurement in bacteria using diethyloxacarbocyanine and a ratiometric technique. Cytometry. 1999; 35:55–63. [PubMed: 10554181]

Appendix A. Supplementary data

Supplementary data related to this article can be found at https://doi.org/10.1016/j.ejmech.2017.10.018.

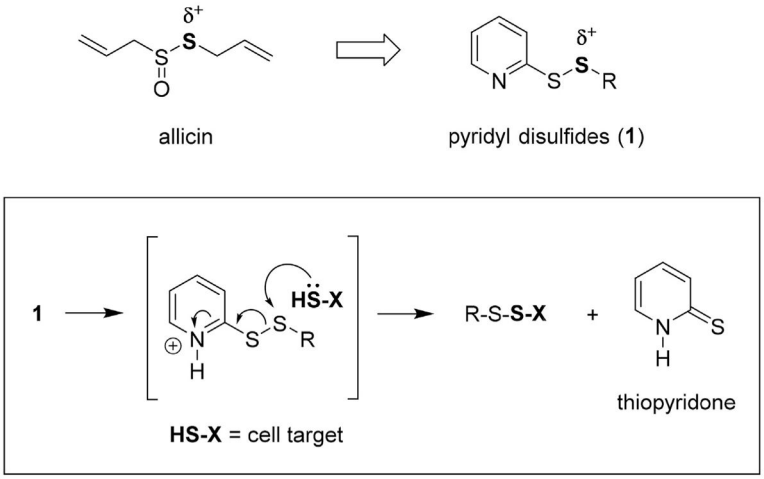

Fig. 1.

Mechanism of the thiol-disulfide exchange reaction for allicin-inspired pyridyl disulfides (**1**).

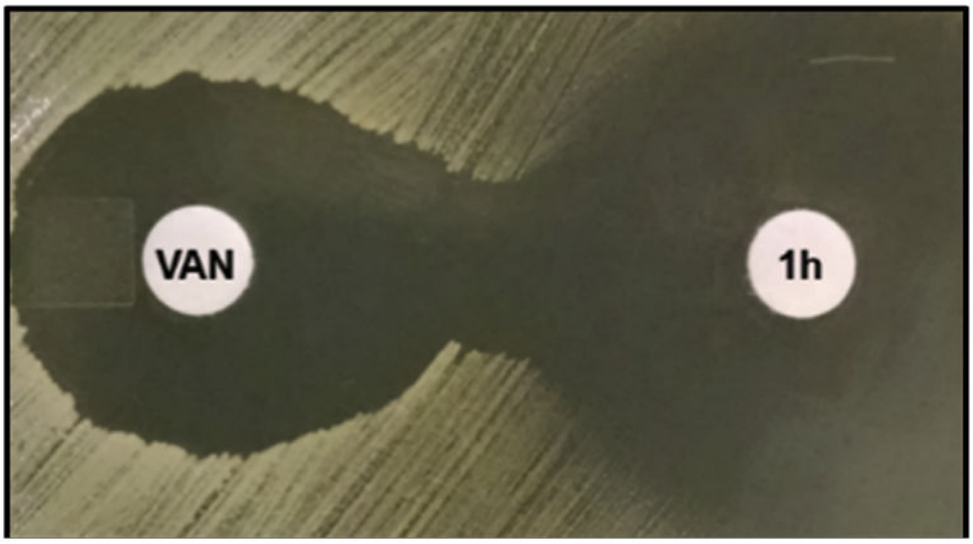

Fig. 2.
Disc diffusion (Kirby-Bauer) assay revealed synergistic activity of pyridyl disulfide **1h** and VAN against MRSA 43300.

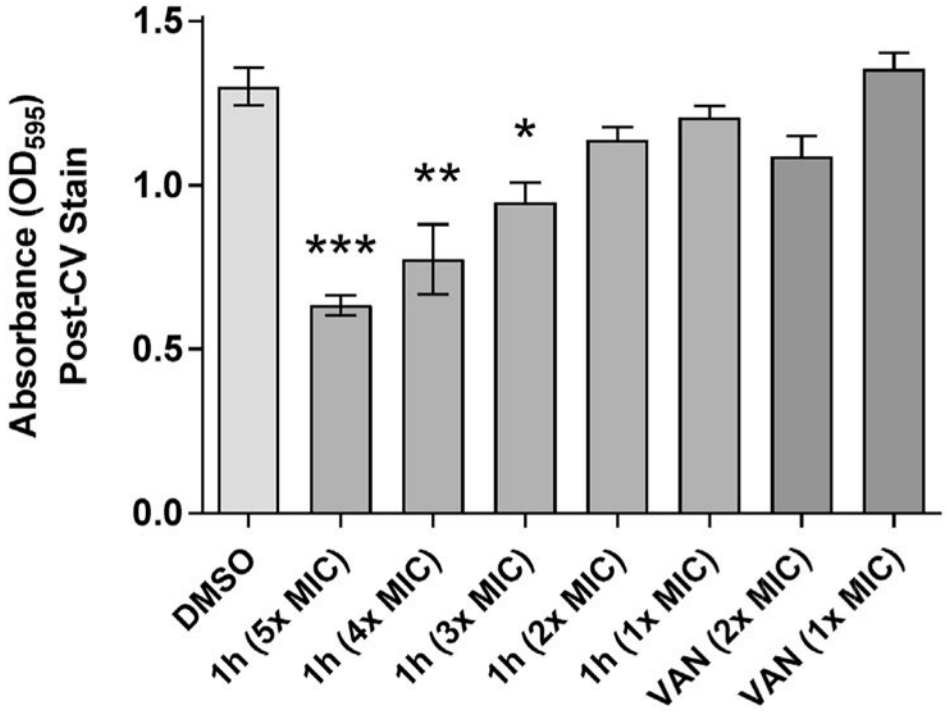

Fig. 3.

Effects of pyridyl disulfide **1h** and VAN on *S. aureus* biofilm dispersal.

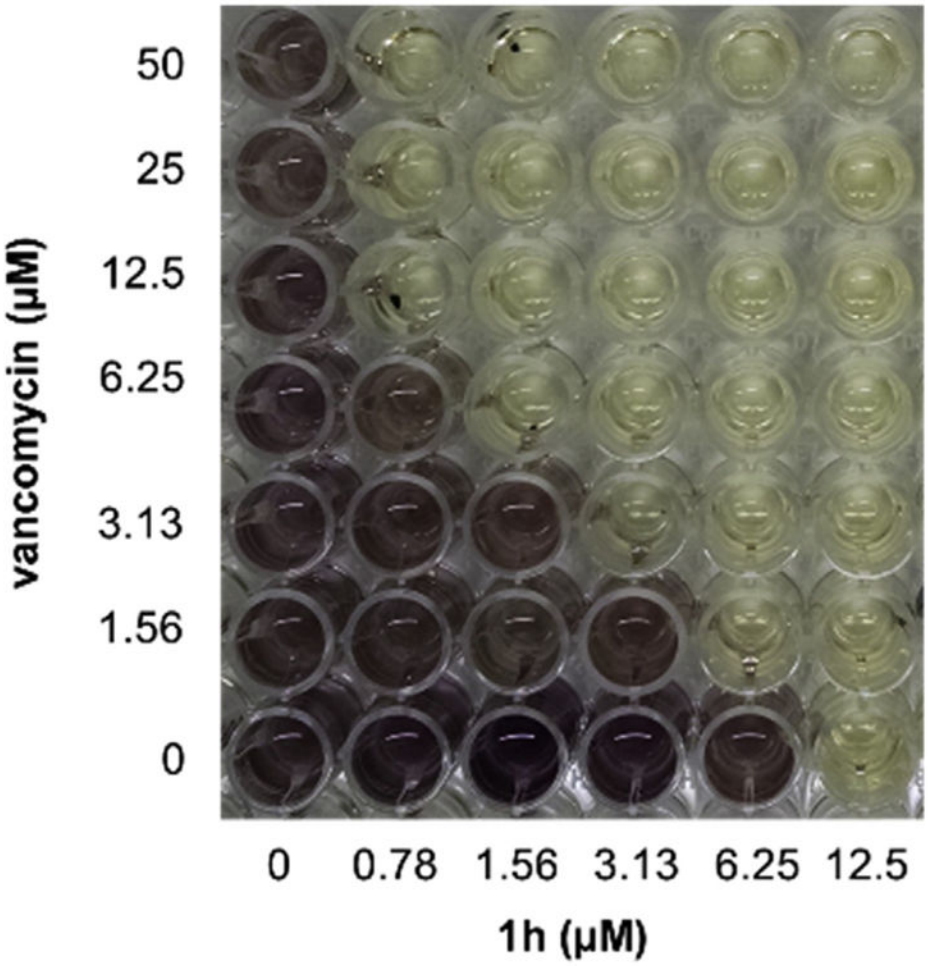

synergy	indifference	antagonism
$\Sigma FIC \leq 0.5$	$0.5 < \Sigma FIC \leq 4$	$4 < \Sigma FIC$
5	0	0

Fig. 4.
The checkerboard assay revealed synergism between vancomycin and disulfide **1h** against VRSA HIP14300.

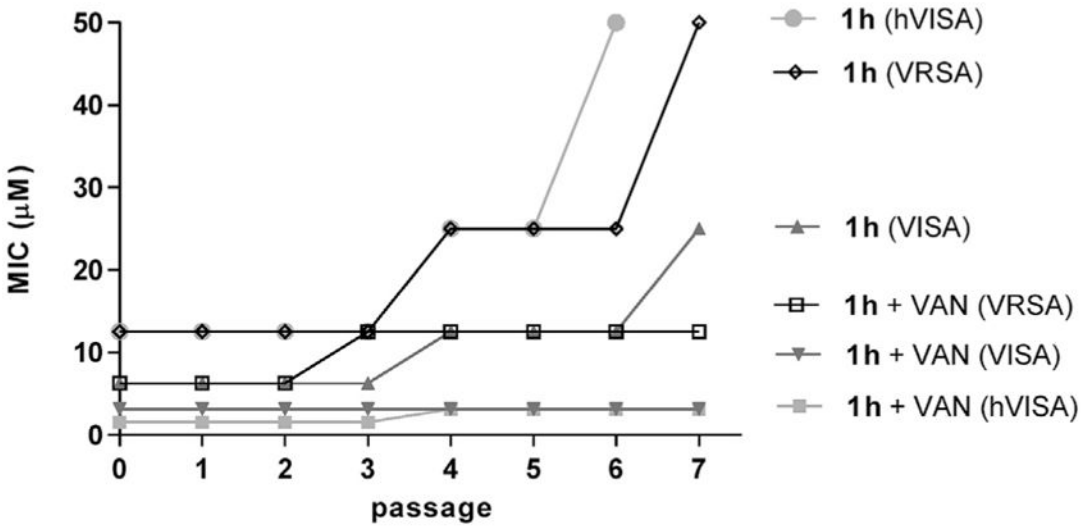

Fig. 5.
Development of resistance by serial passage for disulfide **1h** ± vancomycin.

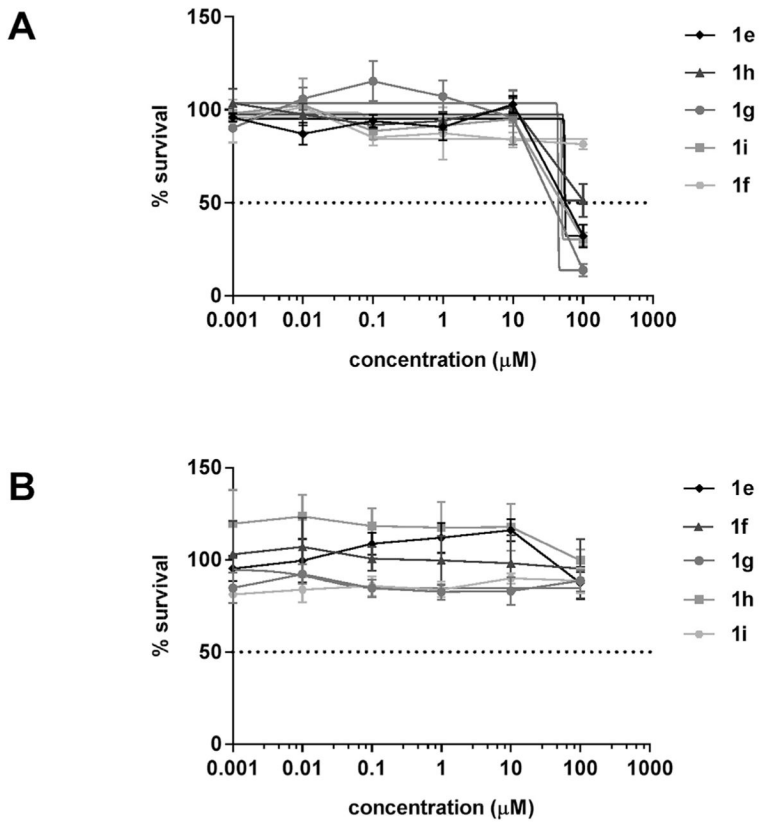

Fig. 6.

Dose response curve of pyridyl disulfide **1e–i** on breast (A) MDA-MB-231 and (B) liver HepG2 carcinoma cell lines.

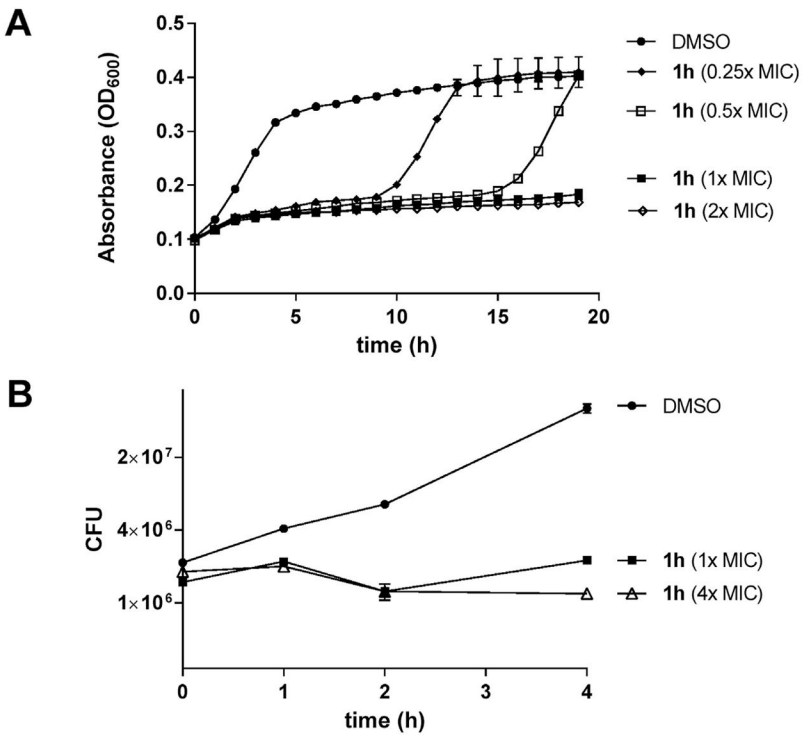

Fig. 7.

Effects of pyridyl disulfide **1h** on growth in MSSA 25923.

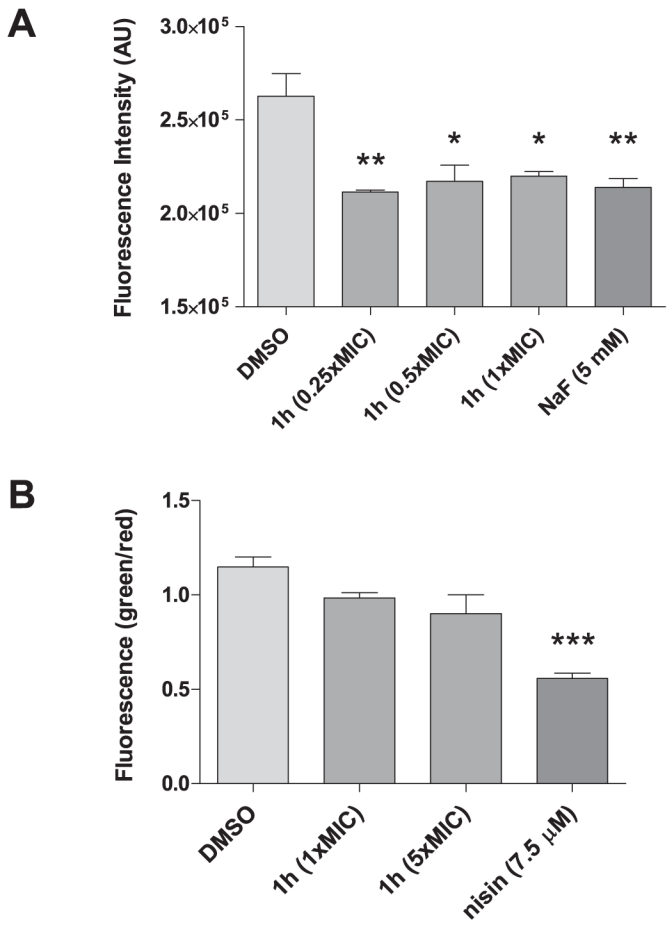

Fig. 8.

Effects pyridyl disulfide **1h** on MSSA 25923 viability. Shown are the (A) C_{12}-resazurin and (B) LIVE/DEAD *Bac*Light™ assays for individual groups depicted as mean ± SEM (n = 3).

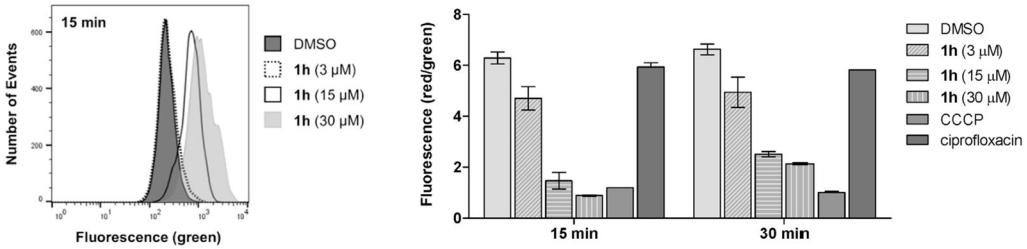

Fig. 9.

Comparative effects on membrane potential. Shown are green fluorescence (left; 530/30 filter) and the ratio of red (585/42 filter) to green fluorescence for individual groups, shown as mean ± SEM (right; n = 2).

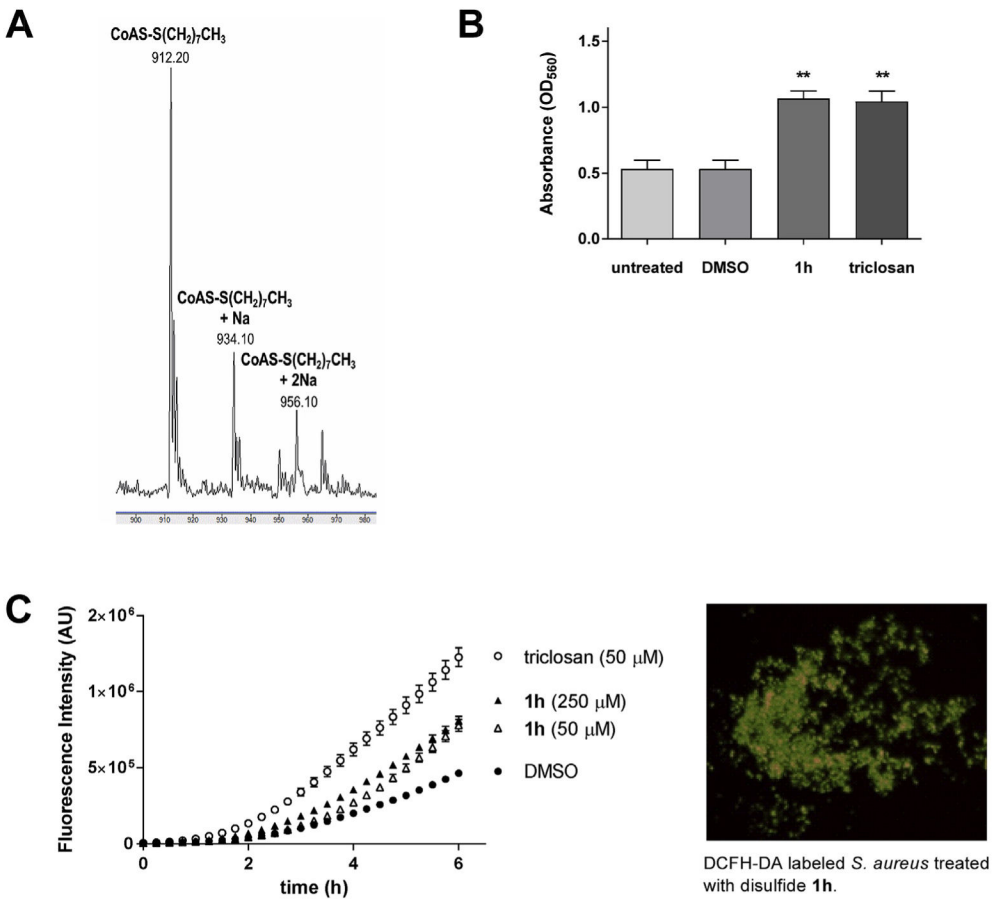

Fig. 10.

Effects of pyridyl disulfides on CoASH and cellular redox state. (A) Mass spectroscopy revealed that *S*-(octylthio)-2-pyridine (**1h**) reacts with coenzyme A (CoASH) *in situ* by thiol-disulfide exchange. (B) Effect of disulfide **1h** in *S. aureus* by nitroblue tetrazolium (NBT) staining. (C) Effect of disulfide **1h** in *S. aureus* by dicholorodihydrofluorescin-diacetate (DCFH-DA) staining.

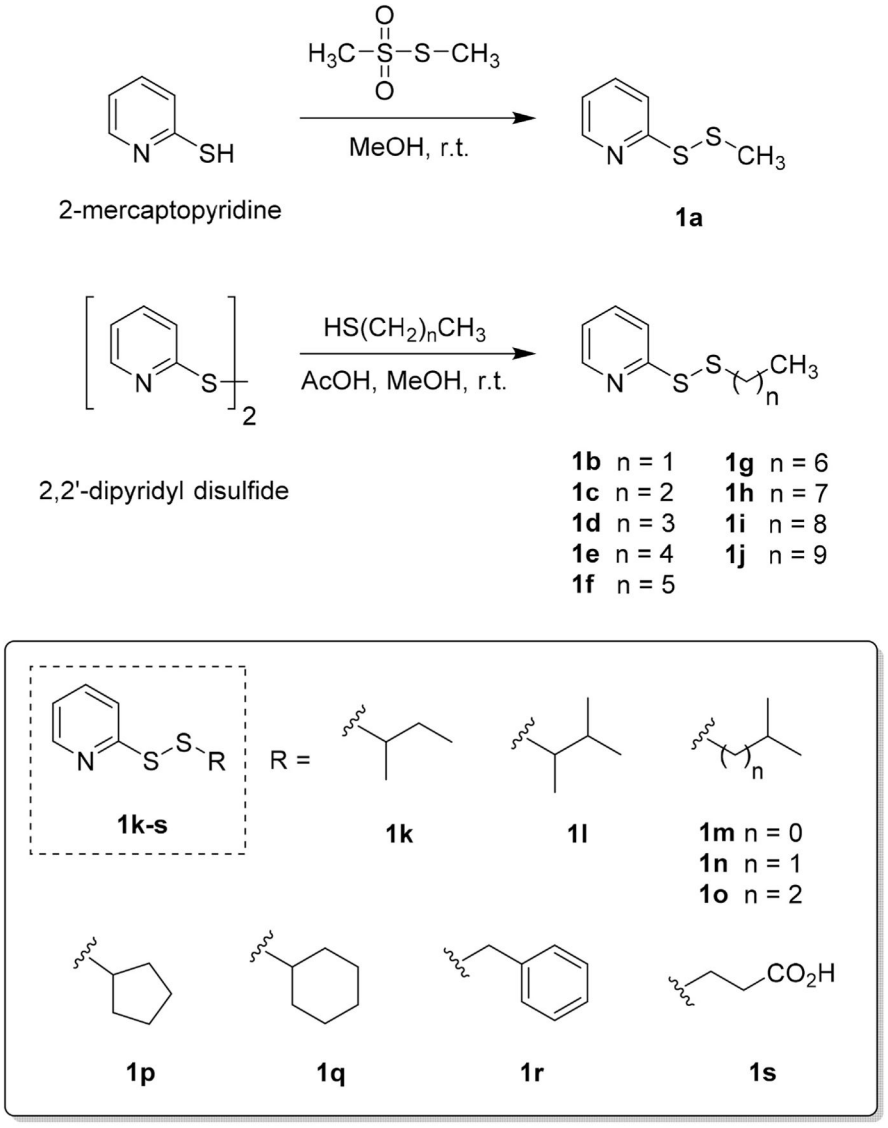

Scheme 1.

Chemical library of synthesized pyridyl disulfides (**1**) used in the study.

Table 1

MIC and MBC data for select disulfides against *S. aureus*.

Species | Strain	Test agent[a]	MIC[a]	MBC[a]	ratio[b]
MSSA ATCC 25923	**1e**	50	–	–
	1f	25	–	–
	1g	12.5	>50	>4:1
	1h	12.5	>50	>4:1
	1i	12.5	>50	>4:1
	VAN	0.78	1.56	2:1
MRSA ATCC 43300	**1e**	50	–	–
	1f	50	–	–
	1g	6.25	>50	>8:1
	1h	6.25	>50	>8:1
	1i	6.25	>50	>8:1
	VAN	0.39	0.78	2:1
LRSA SA LinR#14	**1e**	>50	–	–
	1f	50	–	–
	1g	25	–	–
	1h	25	–	–
	1i	25	–	–
	VAN	0.78	1.56	2:1
hVISA Mu3 ATCC 700698	**1e**	50	–	–
	1f	50	–	–
	1g	12.5	>50	>4:1
	1h	12.5	>50	>4:1
	1i	6.25	>50	>8:1
	VAN	0.78	0.78	1:1
VISA Mu50 ATCC 700699	**1e**	50	–	–
	1f	25	–	–
	1g	3.13	25	8:1
	1h	3.13	25	8:1
	1i	1.56	25	16:1
	VAN	3.13	3.13	1:1
VRSA HIP11714	**1e**	>50	–	–
	1f	50	–	–
	1g	6.25	>50	>8:1
	1h	6.25	>50	>8:1
	1i	12.5	>50	>4:1
	VAN	>50	–	–

[a] Values reported in μM.

[b] MBC:MIC.

Table 2

MIC data for pyridyl disulfide **1e–i** against *S. aureus*.

Variant (no. strains)	Test agent	MIC_{50}[a]	MIC_{90}[a]	Range[a]
VISA (12)	**1e**	50	50	50–>50
	1f	50	50	25–50
	1g	12.5	12.5	3.13–25
	1h	12.5	12.5	3.13–25
	1i	6.25	12.5	1.56–25
	VAN	3.13	3.13	1.56–3.13
VRSA (10)	**1e**	50	50	50–>50
	1f	50	50	25–50
	1g	6.25	12.5	3.13–12.5
	1h	6.25	12.5	3.13–12.5
	1i	6.25	12.5	3.13–12.5
	VAN	>50	>50	12.5–>50

[a]Values reported in μM.

Table 3

Effect of blood components on susceptibility of MSSA 25923.

Additive	MIC (μM)				
	1g	**1h**	**1i**	**OXA**	**VAN**
null	12.5	12.5	12.5	1.56	0.78
glutathione, 100 μM	50	50	50	1.56	0.78
albumin, 0.05% vol/vol	12.5	12.5	25	1.56	0.78
serum, 5% vol/vol	25	25	25	1.56	0.78
serum, 10% vol/vol	25	25	50	1.56	0.78